JOC*Article*

Solvent and Stereoelectronic Effects on the Solvolysis Rates of Oxaspirocyclopropanated 1-Norbornyl Triflates and Related Bridgehead Derivatives

Antonio García Martínez,* Santiago de la Moya Cerero,* Enrique Teso Vilar,† Amelia García Fraile,† Beatriz Lora Maroto, and Cristina Díaz Morillo

Departamento de Química Orgánica I, Facultad de Ciencias Químicas, Universidad Complutense de Madrid, Ciudad Universitaria, 28040 Madrid, Spain

agamar@quim.ucm.es

Received May 6, 2008

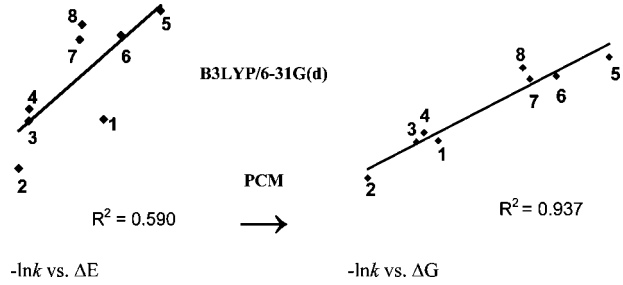

The study of the stereochemical outcome of the solvolysis of oxaspirocyclopropanated 1-norbornyl triflates is highly interesting since these reactions do not lead to the usual retention or fragmentation products but only synthetically interesting rearranged products are enantiospecifically formed. There is no correlation between the experimental solvolysis rates (ln *k*) and the B3LYP/6-31G(d)-computed ionization energies (ΔE) of the corresponding bridgehead hydrocarbons in gas phase. However, this work demonstrates the existence of a fair linear correlation between the experimental reaction rates and the PCM//B3LYP/6-31G(d)-computed free ionization energies in solution (ΔG). This theoretically relevant result reveals that the reason for the lack of linearity in gas phase is not the rearrangement of the intermediate carbocations but unspecific solvent effects on the solvolysis rates, accounted for by the PCM model.

Introduction

Solvent Effects on the Relative Solvolysis Rates of Substituted 1-Norbornyl Triflates. Solvent effects are of paramount importance in organic chemistry.[1] There is a great deal of work dedicated to the experimental study of solvent effects on the solvolysis rate of several substrates, mainly in relation to the Grunwald−Winstein equation,[1,2] but not in the case of Schleyer's relationship of rate constants (ln *k*) vs thermodynamic stability of the involved carbocations in gas phase.[3] Probably due to canceling errors, good relationships are obtained independently of the method used for the definition of the carbocation thermodynamic stability. Originally, this stability was expressed by the difference in strain energy between the bridgehead carbocation and the corresponding hydrocarbon, calculated by molecular mechanics methods.[3] Later, the calculation of strain energies of bridgehead carbocations was based on dissociation energies of the corresponding bromides,[4] isodesmic reactions,[5] or free energies of the proton- or bromide-transfer reactions in the gas phase.[6] The proper state function

* To whom correspondence should be addressed. Phone: +91 3944333. Fax: +91 3944103.

† Facultad de Ciencias, Universidad Nacional de Educación a Distancia (UNED), Senda del Rey 9, 28040 Madrid, Spain.

(1) Reichardt, C. *Solvents and Solvent Effects in Organic Chemistry*; Wiley-VCH: Weinheim, 2002.

(2) (a) Shorter, J. *Correlation Analysis of Organic Reactivity*; Research Studies Press: Chichester, 1982. Also see: (b) Mayr, H.; Ofial, A. R. *Angew. Chem., Int. Ed.* **2006**, *45*, 1844–1854.

(3) (a) For reviews, see: Fort, R. C.; Schleyer, P. v. R. In *Advances in Alicyclic Chemistry*; Academic Press: New York, 1966; Vol. 1, pp 284−370. (b) Fort, R. C.; Schleyer, P. v. R. In *Carbonium Ions*; Wiley-Interscience: New York, 1973; Vol. IV, pp 1783−1835.

(4) For reviews, see: (a) Müller, P.; Mareda, J. In *Cage Hydrocarbons*; Wiley-Interscience: New York, 1990; pp 189−217. (b) Müller, P.; Mareda, J.; Millin, D. *J. Phys. Org. Chem.* **1995**, *8*, 507–528.

(5) (a) Hrovat, D. A.; Borden, W. T. *J. Am. Chem. Soc.* **1990**, *112*, 3277–3228. (b) Della, E. W.; Janowski, W. K. *J. Org. Chem.* **1995**, *60*, 7756–7759.

(6) (a) Müller, P.; Millin, D.; Feng, W. Q.; Houriet, R.; Della, E. W. *J. Am. Chem. Soc.* **1992**, *114*, 6169–6172. (b) Abboud, J. L.; Herreros, M.; Notario, R.; Lomas, J. S.; Mareda, J.; Müller, P.; Rossier, J. C. *J. Am. Chem. Soc.* **1999**, *64*, 6401–6410.

10.1021/jo8009787 CCC: $40.75 © 2008 American Chemical Society
Published on Web 08/06/2008

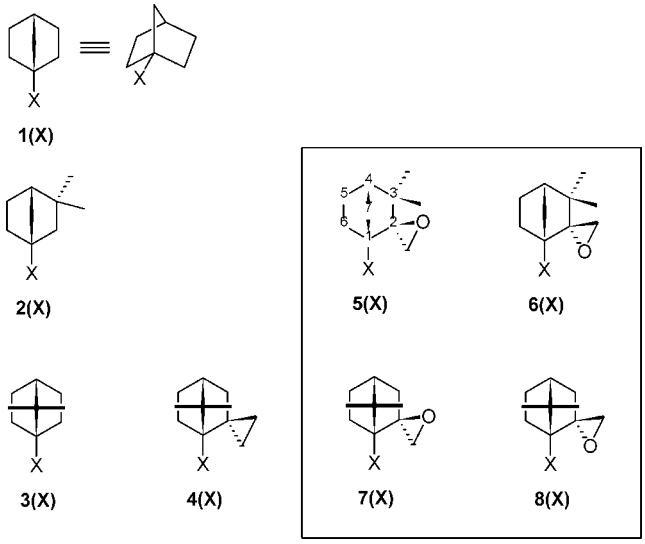

FIGURE 1. Studied 1-norbornyl structures (X = +, H, or OTf).

correlating with ln *k* should be the free energy one, according to the well-known Eyring's equation. However, we have shown that the B3LYP/6-31G(d)-computed free energy differences (ΔG) between bridgehead carbocations and the corresponding hydrocarbons, with both zero-point vibrational energy and thermal corrections (at 298 K, 1 atm), are related by eq 1 to the B3LYP/6-31G(d)-computed total free energy differences (ΔE) without any correction (within an error of ± 0.5 kcal·mol^{-1}), covering a range of ca. 250 kcal·mol^{-1}.[7]

$$\Delta G = \Delta E - 9.1 \quad (1)$$

On the other hand, the relationship quality is very dependent on the solvolysis mechanism. Thus, good linear correlations should be only observed in the case of S_N1 reactions, free from differential solvent-participation effects,[4,8] as well as free from anchimeric (σ-assistance)[9] and F-strain acceleration.[10] Linearity failures have been associated to the formation of rearranged products.[9]

We have reported a fair linear correlation (R^2 = 0.935) between the solvolysis rates and the ΔE values, computed in the gas phase using the DFT B3LYP/6-31G(d) method, for a set of nonrearranging bridgehead 1-norbornyl triflates (i.e., **1(OTf)**, **3(OTf)**, **4(OTf)** in Figure 1) and covering a ln *k* range of ca. 23 units.[11a] In this correlation, an improved R^2 value (0.977) can be reached by excluding substrate **1(OTf)**. This striking result was then attributed to an artifact of the computational method.[11a]

Stereoelectronic Effects on the Solvolysis Rates of 1-Norbornyl Triflates. It is well-known that the formally sp^2-hybridized C_1 atom of 1-norbornyl carbocations tends to adopt a planar geometry. However, such geometry is not possible in the norbornane strained-cage structure. In these nonplanar carbocations, the increased electron demand can be alleviated by σ-stabilization.[7,11a] Additionally, some years ago we reported the striking stereoelectronic effect exerted by the introduction of a spirocyclopropane group adjacent to the charged bridgehead position of a 1-norbornyl cation.[11a] We believe that the introduction of a spirocyclopropane (or oxaspirocyclopropane) group adjacent to the charged bridgehead position should lead to an increase of both strain energy and positive charge at the cationic position (C_1 norbornane position). Both effects would cause a destabilization of the intermediate carbocation, with the consequent rate decrease, despite of the increase of the stabilizing σ-participation.[11a]

SCHEME 1. Unexpected Solvolytic Behavior of Oxaspirocyclopropanated 1-Norbornyl Triflates 5(OTf)−8(OTf) in Refluxing Aqueous Ethanol Buffered with Triethylamine

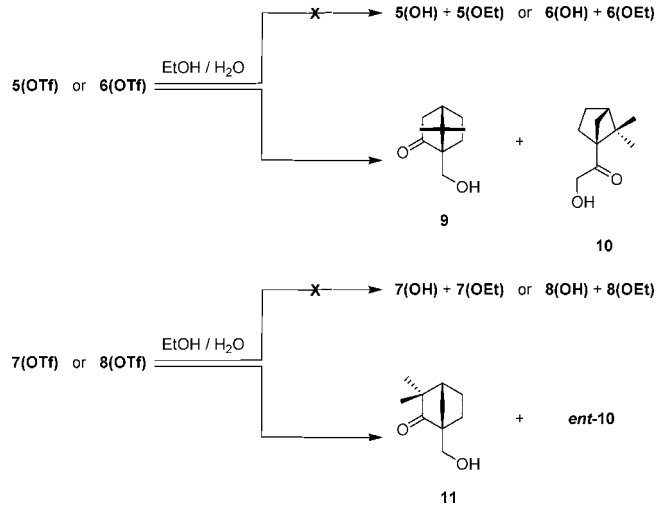

On the basis of above data, we came interested in studying the solvolytic behavior of the oxaspirocyclopropanated 1-norbornyl triflates **5(OTf)−8(OTf)** (Figure 1) in order to gain information on the stereoelectronic effect exerted by the introduction of an oxygen atom in the spirociclopropane group of the **4(OTf)** framework. We are also interested in clarifying the mentioned anomalous behavior of parent **1(OTf)**: a computational artifact or an unexpected solvent effect?

Experimental Results

First results on the solvolysis of the 3,3-dimethylated oxaspirocyclopropanated 1-norbornyl triflates **5(OTf)** and **6(OTf)** (Figure 1) were reported by us in 2001.[12] The solvolysis were then conducted in refluxing aqueous ethanol (60% w/w) buffered with triethylamine.[12] We have now carried out the kinetic study of those reactions and the complete study (solvolytic and kinetic) for the related 7,7-dimethylated oxaspirocyclopropanated 1-norbornyl triflates **7(OTf)** and **8(OTf)** (see Figure 1) under the same reaction conditions. All of the obtained reaction products are shown in Scheme 1. Table 1 shows the corresponding reaction yields.

(7) García Martínez, A.; Teso Vilar, E.; Osío Barcina, J.; de la Moya Cerero, S. *J. Am. Chem. Soc.* **2002**, *124*, 6676–6685.

(8) (a) Abboud, J. L.; Castaño, O.; Dávalos, J. Z.; Jiménez, P.; Gomperts, R.; Müller, P.; Roux, M. V. *J. Org. Chem.* **2002**, *67*, 1057–1060. (b) Abboud, J. L.; Alkorta, I.; Davalos, J.; Müller, P.; Quintanilla, E.; Rossier, J. C. *J. Org. Chem.* **2003**, *68*, 3786–3796.

(9) (a) Wiberg, K. B.; Hadad, C. M.; Sieber, S.; Schleyer, P. v. R. *J. Am. Chem. Soc.* **1992**, *114*, 5820–5828. (b) Adcock, W.; Krstic, A. R. *Tetrahedron Lett.* **1992**, *33*, 7397–7398. (c) Della, E. W.; Grob, C. A.; Taylor, D. K. *J. Am. Chem. Soc.* **1994**, *116*, 6159–6166. (d) Della, E. W.; Schiesser, C. H. *J. Chem. Soc., Chem. Commun.* **1994**, 417–419. (e) Della, E. W.; Janowski, W. K. *J. Chem. Soc., Chem. Commun.* **1994**, 1763–1764. (f) Wiberg, K. B.; McMurdie, N. *J. Am. Chem. Soc.* **1994**, *116*, 11990–11998.

(10) (a) Bentley, T. W.; Roberts, K. *J. Org. Chem.* **1985**, *50*, 5852–5855. (b) Takeuchi, K.; Ohga, Y.; Munakata, M.; Kitagawa, T.; Kinoshita, T. *Tetrahedron Lett.* **1992**, *33*, 3335–3338.

(11) (a) García Martínez, A.; Teso Vilar, E.; de la Moya Cerero, S.; Osío Barcina, J.; Gómez, P. C. *J. Org. Chem.* **1999**, *64*, 5611–5619. (b) Smith, W. G. *J. Org. Chem.* **2001**, *66*, 376–380.

(12) García Martínez, A.; Teso Vilar, E.; García Fraile, A.; de la Moya Cerero, S.; Lora Maroto, B.; Díaz Morillo, C. *Tetrahedron Lett.* **2001**, *42*, 8293–8296.

TABLE 1. Reaction Yields for the Solvolysis of Oxaspirocyclopropanated 1-Norbornyl Triflates 5(OTf)−8(OTf) in Refluxing Aqueous Ethanol Buffered with Triethylamine

	yield (%)				
starting triflate	**9**	**10**	**11**	*ent*-**10**	ref
5(OTf)		78			12
6(OTf)		81			12
7(OTf)			55	14	
8(OTf)			74		

The previously described solvolysis of related 1-norbornyl triflates **1(OTf)−4(OTf)** (Figure 1), under analogous reaction conditions, gave place to the corresponding unrearranged bridgehead alcohols and ethers (60/40 ratio).[11a,13] Unexpectedly, only rearranged alcohols were isolated in the solvolysis of the oxaspirocyclopropanated **5(OTf)−8(OTf)** (see Scheme 1 and Table 1). The formation of such rearranged reaction products could be explained according to the reaction pathways proposed in Scheme 2.

For the kinetic study of our oxaspirocyclopropanated 1-norbornyl triflates, each solvolysis reaction was performed into 12 sealed ampules, which were placed in a thermostatically controlled oil bath at 368.3 K. Typical concentrations are as follows: triflate = 2.5×10^{-2} M, triethylamine = 5.0×10^{-2} M. The solvolysis reaction was monitored by opening the ampules one by one at regular reaction times and subsequent GLC analysis (5-nonanone was used as internal standard for the GLC analysis). The experimental error for the obtained unimolecular rate constants (k) was better than ±5%. Table 2 shows the found k values. Previously reported data for related triflates **1(OTf)−3(OTf)**[13] and **4(OTf)**[11a] have been introduced in Table 2 for comparison. The reported extrapolated values were calculated from k values obtained at three different temperatures in the range 333−373 K.

TABLE 2. Rate Constants (k) for the Solvolysis of 1-Norbornyl Triflates in Buffered (Triethylamine) Aqueous Ethanol (60% w/w) at 368.3 K

triflate	k (s^{-1})	ref
1(OTf)	1.1×10^{-4}[a]	13
2(OTf)	1.2×10^{-3}[a]	13
3(OTf)	1.2×10^{-4}[a]	13
4(OTf)	6.7×10^{-5}[a]	11a
5(OTf)	5.5×10^{-7}	
6(OTf)	1.8×10^{-6}	
7(OTf)	2.3×10^{-6}	
8(OTf)	1.1×10^{-6}	

[a] Extrapolated values.

Computational Methods

The three-parameter hybrid generalized gradient approximation (GGA) functional B3LYP is one of the most popular tools in computational chemistry. However, it has unsatisfactory performance issues, such as its tendency to underestimate the computation of barrier heights by an average of ca. 4 kcal·mol^{-1}.[14] However, it should be noticed that functionals are approximate and there will always be cases where they afford good results. Thus, we have shown that the low-level B3LYP/6-31G(d) method affords ionization energies for bridgehead hydrocarbons in the gas phase (ΔE) which are in very good accordance with the corresponding solvolysis rates in aqueous ethanol, and covering a ln k range of 23 units (see above).[11a] Moreover, the B3LYP/6-31G(d) method seems to be good enough for computing reactions involving carbocations.[5a,11b] On the base of these facts, we have considered convenient to continue using the computationally inexpensive B3LYP/6-31G(d) method for this work.

Thus, for the computation of the total energies (E) in gas phase, without any corrections, of hydrocarbons and carbocations **1(X)−8(X)** (X = H or +, respectively, see Figure 1), alcohols **9−11** (see Scheme 1) and intermediates **12−18** (see Scheme 2), the B3LYP/6-31G(d) method implemented in the GAUSSIAN 03 package of programs was used (Chem3D was chosen as graphical interface).[15]

For the study of unspecific solvent effects on the relative solvolysis rates, we have used the polarizable continuum model (PCM)[16a] of the self-consistent reaction field theory (SCRF),[16b] as implemented in GAUSSIAN 03. The PCM affords the total free energy in solution (G), including nonelectrostatic terms. Hence, the PCM model at the B3LYP/6-31G(d) theoretical level, in combination with eq 1, offers a very easy tool for the computation of the change in free energy for the transfer of carbocations and neutral species from gas phase to solution. These transfer energies are difficult to calculate using procedures based in thermodynamic cycles.[17] The PCM//B3LYP/6-31G(d) method was the key for the interpretation of the striking methyl effect on the solvolysis rates of bridgehead derivatives.[7] Moreover, this method has been successfully used for the computation of the potential energy surface for the solvolysis of 1-adamantyl, *tert*-butyl, and methyl chlorides.[18]

We have fixed the scaling factor α as 1.2 and the number of tesserae on each sphere as 60 for the description of the atomic spheres. The transition states (TS) for the alternative reaction pathways in the gas phase were located with the IRC and TS facilities implemented in GAUSSIAN 03. All the computed TSs ($\Delta E^{\ddagger}$) exhibited one imaginary frequency. The corresponding free energies of activation ($\Delta G^{\ddagger}$) were calculated with the PCM model. Unfortunately, we have renounced to the computation of the $\Delta G^{\ddagger}$ values in the case of intramolecular hydrogen-transfer processes (see steps IV in Scheme 2), due to the lack of convergence in solution.

The computed E and G values at the solvolysis temperature are given in Table 3.

(13) García Martínez, A.; Osío Barcina, J.; Rodríguez Herrero, M. E.; Iglesias de Dios, M. I.; Teso Vilar, E.; Subramanian, L. R. *Tetrahedron Lett.* **1994**, *35*, 7285–7288.

(14) Zhao, Y.; González-García, N.; Truhlar, D. G. *J. Phys. Chem. A* **2005**, *109*, 2012–2018.

(15) (a) Frisch, M. J.; Trucks, G. W.; Schlegel, H. B.; Scuseria, G. E.; Robb, M. A.; Cheeseman, J. R.; Zakrzewski, V. G.; Montgomery, J. A.; Stratmann, R. E.; Burant, J. C.; Dapprich, S.; Millam, J. M.; Daniels, A. D.; Kudin, K. N.; Strain, M. C.; Farkas, O.; Tomasi, J.; Barone, V.; Cossi, M.; Cammi, R.; Mennucci, B.; Pomelli, C.; Adamo, C.; Clifford, S.; Ochterski, J.; Petersson, G. A.; Ayala, P. Y.; Cui, Q.; Morokuma, K.; Malick, D. K.; Rabuck, A. D.; Raghavachari, K.; Foresman, J. B.; Cioslowski, J.; Ortiz, J. V.; Baboul, A. G.; Stefanov, B. B.; Liu, G.; Liashenko, A.; Piskorz, P.; Komaromi, I.; Gomperts, R.; Martin, R. L.; Fox, D. J.; Keith, T.; Al-Haman, M. A.; Peng, C. Y.; Nanayakkara, A.; González, C.; Challacombe, M.; Gill, P. M. W.; Johnson, B.; Chen, W.; Wong, M. W.; Andres, J. L.; Head-Gordon, M.; Replogle, E. S.; Pople, J. A. Gaussian 98W; Gaussian Inc.: Pittsburgh, PA, 1998. Licensed to García Martínez, A. (b) Chem3D v. 8.0. Cambridgesoft, Cambridge, MA, 2002. Licensed to García Martínez, A.

(16) (a) Miertus, S.; Tomasi, J. *J. Chem. Phys.* **1982**, *65*, 239–252. (b) Tomasi, J.; Persico, M. *Chem. Rev.* **1994**, *94*, 2027–2094.

(17) Herrero, R.; Quintanilla, E.; Müller, P.; Abboud, J. L. *Chem. Phys. Lett.* **2006**, *420*, 493–496.

(18) García Martínez, A.; Teso Vilar, E.; Osío Barcina, J.; de la Moya Cerero, S. *J. Org. Chem.* **2005**, *70*, 10238–10246.

SCHEME 2. Proposed Competitive Reaction Pathways for the Solvolysis of Triflates 5(OTf)−8(OTf) in Aqueous Ethanol[a]

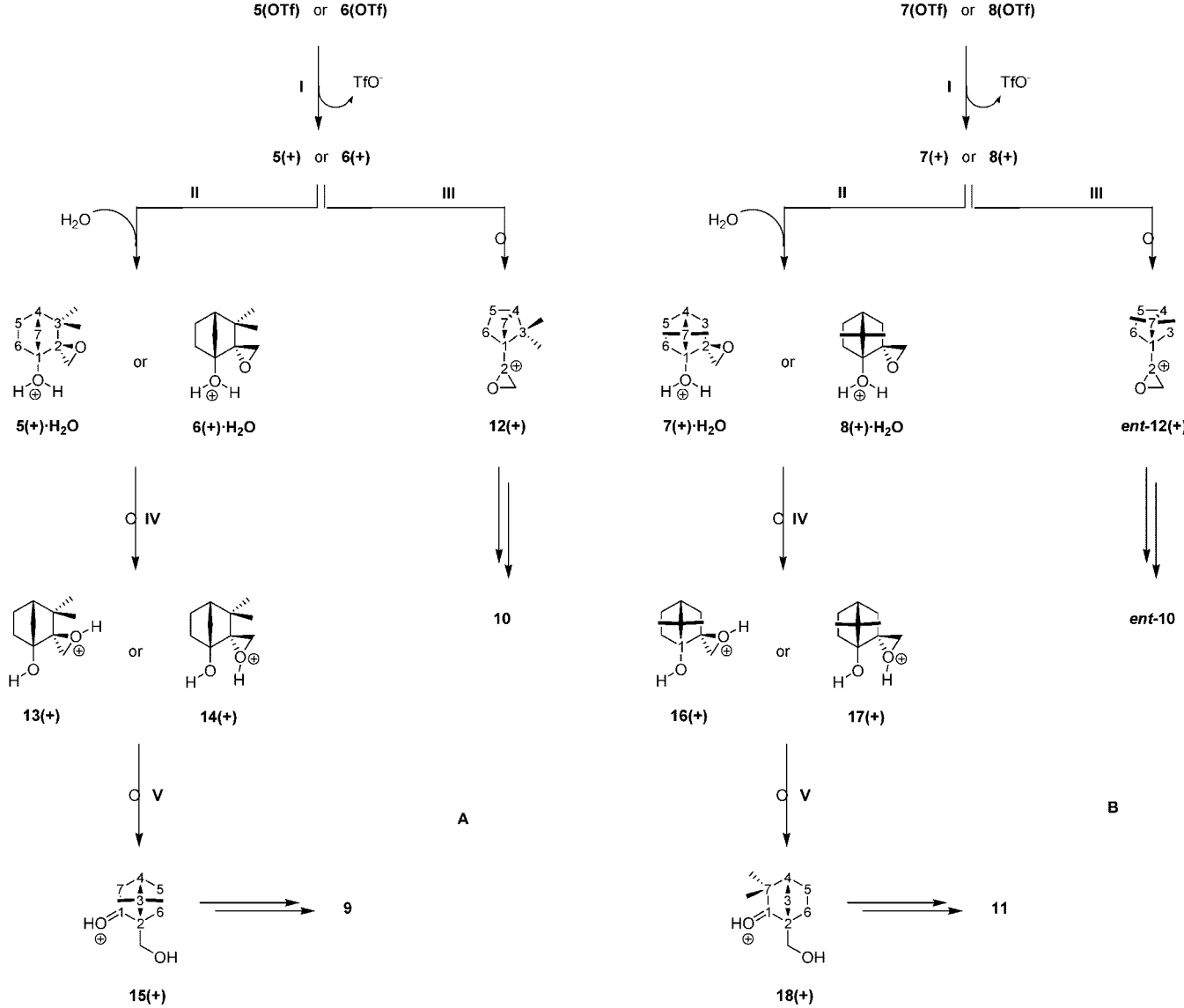

[a] Key: (I) ionization; (II) trapping by water; (III) C_2-C_3-to-C_2-C_1 Wagner−Meerwein rearrangement; (IV) O-to-O proton transfer; (V) protonated-epoxide-induced C_6-C_1-to-C_6-C_2 pinacol-type rearrangement.

Discussion

The ionization ΔE values for hydrocarbons **1(H)**−**8(H)** were calculated from the computed data reported in Table 3. These ionization energies (ΔE[(+)-**(H)**]) are shown in Table 4.

The found ionization energies for the oxaspirocyclopropanated hydrocarbons **5(H)**−**8(H)** are higher than the calculated one for the spirocyclopropanated parent hydrocarbon **4(H)** (see Table 4). In relation to this, it is known that the substitution of a methylene group of the cyclopropane moiety by an oxygen atom causes a decrease of the strain energy. Thus, the experimental heat of hydrogenation of cyclopropane to propane (−37.06 kcal·mol^{-1}) is higher than the corresponding value for the reduction of oxirane to dimethyl ether (−31.41 kcal·mol^{-1}).[19] This decrease in strain energy (5.6 kcal·mol^{-1}) agrees with the value computed by us for such a case using the B3LYP/6-31G(d) method (6.4 kcal·mol^{-1}). However, in our norbornane-based cases, the introduction of an oxygen atom in the spiranic group causes an increase in the positive charge at the C_2 atom of the norbornane moiety (spiranic carbon). This last effect should be the responsible of the higher ΔE values computed for hydrocarbons **5(H)**−**8(H)**, in relation to the computed one for **4(H)** (Table 4).

As mentioned above, the higher electron demand of the cationic C_1 atom could be partially satisfied by the σ-assistance of the norbornane cage. In order to detect such σ-assistance, we have studied the computed inherent geometrical distortions and Mullikan charges in our 1-norbornyl carbocations. The more relevant interatomic distances and Mullikan charges of carbocations **1**(+), **3**(+), and **4**(+) have been previously reported by us.[11a] Figure 2 shows data for the previously computed spirocyclopropanated carbocation **4**(+)[11a] and the now-computed oxaspirocyclopropanated carbocations **5**(+)−**8**(+).

The structures given in Figure 2 show the greatest variation in σ-assistance described so far for the 1-norbornyl system (detailed geometrical data are available in the Supporting

(19) Afeefy, H., Liebman, J., Stein, S. NIST Standard Reference Database; Gaithersburg, MD, 2005.

TABLE 3. Selected Calculated Energies (in Hartrees) in Both Gas Phase (*E*) and Solution (*G*) at 368.3 K

structure	*E*	*G*
1(X)	−273.96849 (X = H)	−273.95764 (X = H)
	−273.04073 (X = +)	−273.09664 (X = +)
2(X)	−352.59349 (X = H)	−352.57711 (X = H)
	−351.67648 (X = +)	−351.72194 (X = +)
3(X)	−352.59094 (X = H)	−352.57483 (X = H)
	−351.67263 (X = +)	−351.71563 (X = +)
4(X)	−429.97525 (X = H)	−429.95616 (X = H)
	−429.05687 (X = +)	−429.09635 (X = +)
5(X)	−465.87772 (X = H)	−465.86143 (X = H)
	−464.94299 (X = +)	−464.98628 (X = +)
6(X)	−465.87778 (X = H)	−465.86134 (X = H)
	−464.94800 (X = +)	−464.99058 (X = +)
7(X)	−465.87653 (X = H)	−465.85991 (X = H)
	−464.95191 (X = +)	−464.99135 (X = +)
8(X)	−465.87630 (X = H)	−465.85972 (X = H)
	−464.95117 (X = +)	−464.99174 (X = +)
9	−541.13179	−541.12709
10	−541.09476	−541.07733
11	−541.13427	−541.11800
5(+)·H$_2$O	*a*	*a*
6(+)·H$_2$O	−541.40899	−541.46324
7(+)·H$_2$O	−541.42107	−541.47052
8(+)·H$_2$O	−541.40788	−541.46060
12(+)	−464.95449	−465.01097
13(+)	−541.43828	-541.49956
14(+)	−541.42992	−541.49472
15(+)	−541.48615	−541.54565
16(+)	−541.43565	−541.49647
17(+)	−541.42896	−541.49801
18(+)	−541.49069	−541.53395
TS[5(+) to 12(+)]	−464.94227	−464.98479
TS[6(+) to 12(+)]	−464.94412	−464.98567
TS[6(+)·H$_2$O to 14(+)]	−541.40146	*b*
TS[13(+) to 15(+)]	−541.43772	−541.49775
TS[14(+) to 15(+)]	−541.28890	−541.35151
TS[7(+) to *ent*-12(+)]	−464.93330	−464.97496
TS[8(+) to *ent*-12(+)]	−464.93330	−464.97496
TS[7(+)·H$_2$O to 16(+)]	−541.42086	*b*
TS[8(+)·H$_2$O to 17(+)]	−541.40146	*b*
TS[16(+) to 18(+)]	−541.43556	−541.49612
TS[17(+) to 18(+)]	−541.42895	−541.49794

[a] Attempts to optimize this structure afford structure **13**(+). [b] No convergence was achieved in solution.

TABLE 4. Experimentally Calculated Rates (−ln *k*) for the Solvolysis of 1-Norbornyl Triflates 1(OTf)−8(OTf) as well as B3LYP/6-31G(d)-Calculated Ionization Energies in the Gas Phase (Δ*E*) and PCM//B3LYP/6-31G(d)-Calculated Ionization Energies in Solution (Δ*G*) for the Corresponding Hydrocarbons (Energies in kcal·mol^{-1})

triflate	ln *k*[a]	Δ*E*[#(+)-#(H)]	Δ*G*[#(+)-#(H)]
1(OTf)	9.11	582.10	540.28
2(OTf)	6.72	575.46	536.63
3(OTf)	9.03	576.24	539.15
4(OTf)	9.61	576.30	539.54
5(OTf)	14.4	586.55	549.17
6(OTf)	13.2	583.45	546.41
7(OTf)	13.0	580.21	545.03
8(OTf)	13.7	580.41	544.67

[a] Values at 368.3 K.

Information). Particularly striking is the σ-participation of the corresponding C_4-C_7 bond, which is nearly coplanar with the p-orbital of the formally sp^2-hybridized C_1 carbons in the 7,7-dimethylated systems (see structures **7**(+) and **8**(+) in Figure 2). This bond is lengthened to ca. 2.4 Å (!) and the C_1-C_7 bond shortened to ca. 1.4 Å (!).

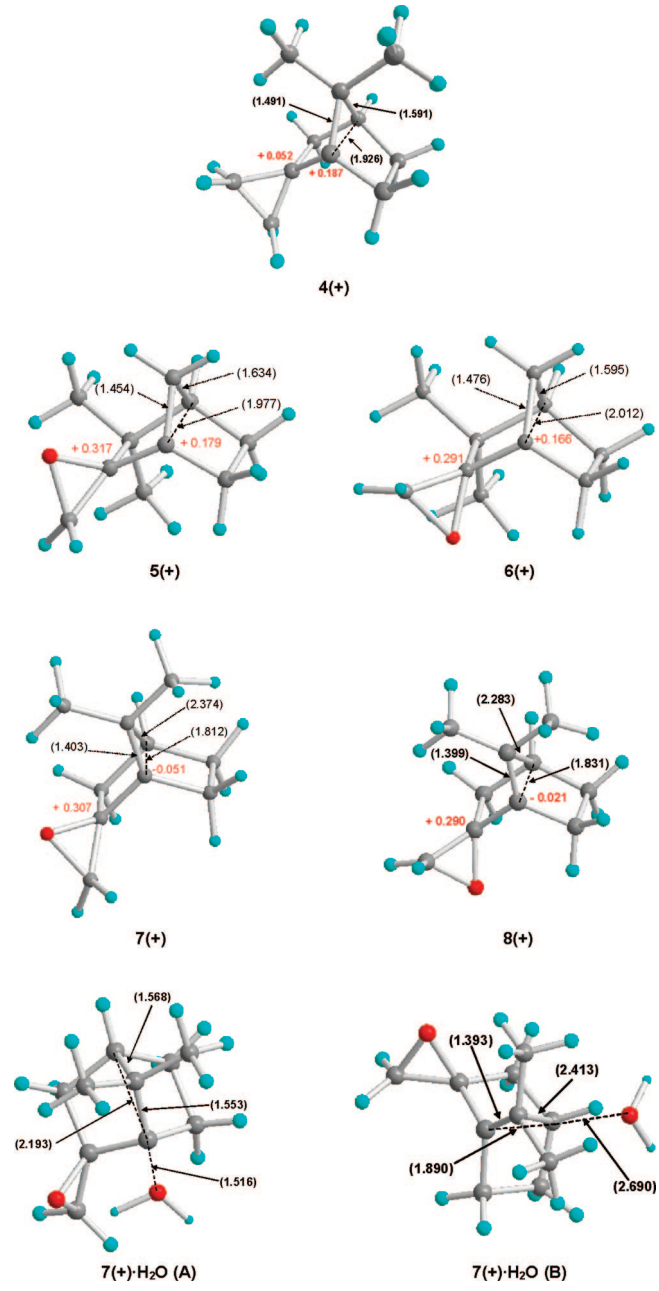

FIGURE 2. B3LYP/6-31G(d)-computed geometries for bridgehead 1-norbornyl carbocations **4**(+)−**8**(+) and **7**(+)·**H$_2$O**. Selected distances into parentheses (in Å) and Mulliken charges in red (in au).

The σ-assistance is also reflected in the flattening of the bridgehead carbocations. This flattening can be measured by the degree of pyramidalization (ϕ) of the bridgehead cation, calculated by eq 2. This equation is based on the analogous one proposed for the determination of the pyramidalization of alkene systems.[20]

$$\cos\phi = -\cos[(C_7 - C_1 - C_6 + C_7 - C_1 - C_2)/2]/\cos[1/2(C_2 - C_7 - C_6)] \quad (2)$$

Table 5 reproduces the calculated ϕ values for carbocations **4**(+)−**8**(+), showing that **7**(+) is the most flattened bridgehead 1-norbornyl carbocation described so far.

On the other hand, a very poor linear correlation ($R^2 = 0.590$), between the calculated ionization energies for the bridgehead 1-norbornyl hydrocarbons in gas phase (Δ*E*[#(+)−#(H)]) and

TABLE 5. Selected B3LYP/6-31G(d)-Computed Angles and Degree of Pyramidalization (ϕ) (Both in Degrees) for Bridgehead 1-Norbornyl Carbocations 4(+)−8(+)

cation	$C_7-C_1-C_6$	$C_7-C_1-C_2$	$C_2-C_7-C_6$	ϕ
4(+)	112.4	116.1	118.4	36.7
5(+)	112.0	113.0	120.8	39.2
6(+)	111.1	115.0	119.1	39.4
7(+)	122.3	123.8	113.6	5.2
8(+)	121.9	124.2	112.7	10.2

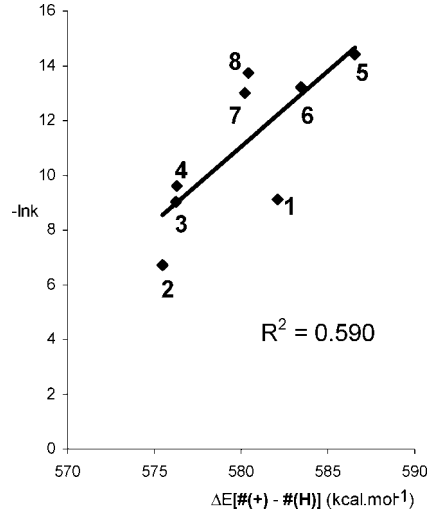

FIGURE 3. Linear correlation between B3LYP/6-31G(d)-calculated ΔE [**#**(+)−**#(H)**] and ln *k*.

the experimental solvolysis rates (ln *k*) of the corresponding 1-norbornyl triflates, was found (Table 5 and Figure 3).

The reason for the lack of linearity seems to be not due to the inclusion of the rearranging oxaspirocyclopropanated triflates **5(OTf)**−**8(OTf)**, since the dispersion also affects to the non-rearranging triflates **1(OTf)**−**4(OTf)**.

In order to determine the nature of the lack of linear correlation in gas phase, we calculated the corresponding ionization ΔG values, computed with the PCM//B3LYP/6-31G(d) method at the solvolysis conditions (see Table 4), finding now a fair linear correlation ($R^2 = 0.937$) of ΔG vs $-\ln k$ (Figure 4).

The comparison between Figures 3 and 4 suggests that the main reasons for the lack of linear correlation for the gas-phase calculation are differential unspecific solvent effects on the

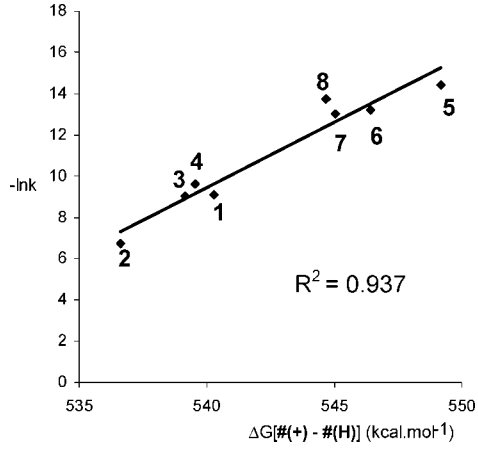

FIGURE 4. Linear correlation between PCM//B3LYP/6−31G(d) calculated ΔG [**#**(+)-**#(H)**] and ln *k*.

TABLE 6. PCM Analysis of Unspecific (SCRF) Solvation Effects (in kcal·mol^{-1}) on *G* Values for Systems 1(H), 1(+), 5(H), 5(+), 8(H), and 8(+)

effect[a]	1(H)	1(+)	5(H)	5(+)	8(H)	8(+)
PS-S	−0.08	−42.5	−1.5	−39.9	−1.6	−38.8
cav	19.5	19.6	27.0	27.4	27.3	28.2
dis	−13.5	−12.9	−16.2	−15.7	−16.3	−15.7
rep	0.79	0.69	0.74	0.66	0.74	0.68
TNE	6.8	7.5	11.37	12.3	11.7	13.14

[a] Electrostatic term: (polarized-solute)−solvent (PS−S) interaction. Non-electrostatic effects: cavitation (cav); dispersion (dis); repulsion (rep), and total non-electrostatic effects (TNE).

intermediate carbocations, mainly on **1**(+) and **2**(+). In order to study the grounds for the differential solvation, we have analyzed the contribution of unspecific solvation effects for hydrocarbons **1(H)**, **5(H)** and **8(H)** and for the corresponding carbocations **1**(+), **5**(+), and **8**(+), in terms of the PCM solvation theory implemented in GAUSSIAN 03. The components of the total free energy (*G*) in aqueous ethanol (60% w/w) at 368.3 K, according to the PCM analysis,[16] are reproduced in Table 6.

The data reported in Table 6 show that the higher stabilization in solution for cation **1**(+) (and **2**(+)), in relation to the oxaspirocyclopropanated cations, is mainly due to the strong stabilizing electrostatic PS-S term, combined with a small relative destabilization due to the nonelectrostatic terms. Therefore, at this calculation level, it is clearly revealed that the lack of linearity observed in gas phase is due neither to differential σ-participation degrees nor deficiencies of the B3LYP/6-31G(d) method but to differential solvent effects. Moreover, it can be also concluded that the solvolysis of the rearranging oxaspirocyclopropanated triflates occurs following the same mechanism. This mechanism seems to be similar to the computed by us for the solvolysis of 1-adamantyl chloride, consisting of the front-side water attack to a carbocation formed under combined nucleophilic and electrophilic solvent assistance (NSA + ESA mechanism).[18]

The activation energies for the individual reaction steps proposed in Scheme 2 can be calculated from the data reported in Table 2. These activation energies are shown in Table 7.

The computed activation energies agree (qualitatively) with the obtained reaction products in the case of the solvolysis of the 7,7-dimethylated oxaspirocyclopropanated 1-norbornyl triflates **7(OTf)** and **8(OTf)**. Thus, in these cases, the water trapping of the initially formed bridgehead carbocations **7**(+) and **8**(+) (see Scheme 2B, step II) takes place faster than the corresponding Wagner−Meerwein rearrangement to ***ent*-12** (see Scheme 2B, step III). Subsequent O-to-O proton transfer (see Scheme 2B, step IV) gives the corresponding protonated epoxides **16**(+) and **17**(+). Note the low activation energies for step IV (entries 13 and 14 in Table 7) in comparison with the higher values for step III (entries 9 and 10 in Table 7). Finally, the pinacol-type rearrangement of these protonated epoxides (see Scheme 2B, step V) and subsequent deprotonation gives way to keto alcohol **11**, which is the main product for the solvolysis of **7(OTf)** and the only isolated product in the case of **8(OTf)** (see Scheme 1 and Table 1).

However, some discrepancies between the calculated energetic barriers and the obtained products are observed for the solvolysis of the 3,3-dimethylated oxaspirocyclopropanated 1-norbornyl triflates **5(OTf)** and **6 (OTf)**. The more important discrepancy is found for **5**(**OTf**). In this case, calculation predicts

TABLE 7. Selected B3LYP/6-31G(d)-Calculated Activation Energies in the Gas Phase ($\Delta E^{\ddagger}$) and PCM//B3LYP/6-31G(d) -Calculated Activation Energies in Solution ($\Delta G^{\ddagger}$, at 368.3 K (Energies in kcal·mol^{-1})

entry	reaction step	$\Delta E^{\ddagger}$	$\Delta G^{\ddagger}$
1	**5**(+) to **12**(+)	0.4	0.9
2	**6**(+) to **12**(+)	2.4	3.1
3	**5**(+) to **5**(+)·$\mathbf{H_2O}$[a]		
4	**6**(+) to **6**(+)·$\mathbf{H_2O}$[a]		
5	**5**(+)·$\mathbf{H_2O}$ to **13**(+)	0.0[b]	0.0[b]
6	**6**(+)·$\mathbf{H_2O}$ to **14**(+)	4.7	[c]
7	**13**(+) to **15**(+)	2.4	0.0
8	**14**(+) to **15**(+)	129.1	89.9
9	**7**(+) to ***ent*-12**(+)	11.7	10.3
10	**8**(+) to ***ent*-12**(+)	11.2	10.5
11	**7**(+) to **7**(+)·$\mathbf{H_2O}$[a]		
12	**8**(+) to **8**(+)·$\mathbf{H_2O}$[a]		
13	**7**(+)·$\mathbf{H_2O}$ to **16**(+)	0.1	[c]
14	**8**(+)·$\mathbf{H_2O}$ to **17**(+)	4.0	[c]
15	**16**(+) to **18**(+)	0.1	0.2
16	**17**(+) to **18**(+)	0.0	0.0

[a] The corresponding hydrated carbocation is formed directly from the front-side substitution. [b] Assumed to be cero, due to the instability of carbocation **5**(+)•$\mathbf{H_2O}$. [c] No-convergence was achieved using the PCM model.

products **9** and **10** to be formed in similar yields (compare the similar energies for entries 1 and 5 in Table 7), which is in contradiction with the obtained results (see Scheme 1 and Table 1). This discrepancy can be explained as follows: the rearrangement of the intermediate carbocation occurs at (or near) the TS, but the water trapping[21] takes place faster for the rearranged carbocation **12**(+) than for the bridgehead carbocations **5**(+) and **6**(+), giving rise to the major formation of the product derived from **12**(+) (i.e., the observed ketoalcohol **10**).

Another striking feature is the very different activation energies for the reactions of carbocations **5**(+)·$\mathbf{H_2O}$ and **6**(+)·$\mathbf{H_2O}$. Thus, cation **5**(+)·$\mathbf{H_2O}$ should be very unstable, since the attempts to optimize its structure afford protonated epoxide **13**(+) (see Table 3). Moreover, our calculations indicate that the pinacol-type rearrangement of **13**(+) to **15**(+) (step V in Scheme 2A) takes place in solution without noticeable activation energy (see entry 7 in Table 7). However, this is not the case for the solvolysis of the epimer cation **6**(+)·$\mathbf{H_2O}$ (see entry 8). The easy both intramolecular O-to-O proton transfer and subsequent pinacol-type rearrangement for the case of **5**(+)·$\mathbf{H_2O}$, when compared with **6**(+)·$\mathbf{H_2O}$, are due to a favored hydrogen bonding (see structure in the Supporting Information) and a higher assistance of the C_1-C_6 bond to the fragmentation of the *exo*-C−O bond, respectively. Additionally, the very easy Wagner−Meerwein rearrangement (ring-contraction) of carbocations **5**(+) and **6**(+), when compared with carbocations **7**(+) and **8**(+) (see the activation energies for entries 1−2 and 9−10 in Table 7) can be attributed to the σ-assistance of the tetrasubstituted C_2-C_3 bond.

Finally, in the cases of carbocations **7**(+) and **8**(+), the tetrasubstitued C_4-C_7 bond is also able to give place to a strong σ-assistance, which is manifested in the flattening of the corresponding bridgehead carbocations (see the corresponding geometries in Figure 2 and degree of pyramidalization in Table 5). Curiously, this σ-assistance does not lead to C−C fragmentation products, and only products with retention of the C_4-C_7 bond were obtained (see Scheme 1 and Table 1). This experimental fact is fairly confirmed by our computations using the B3LYP/6-31G(d) method. Thus, there is no reaction between carbocation **7**(+) and a water molecule located near (under or over) the C_4 atom, whereas the water attack to the C_1 atom leads to **7**(+)·$\mathbf{H_2O}$ under pyramidalization of the bridgehead atoms.

(20) (a) Borden, W. T. *Chem. Rev.* **1989**, *89*, 1095–1109. (b) Williams, R. V. *J. Org. Chem.* **2004**, *69*, 7134–7142.
(21) Jenks, W. P. *Acc. Chem. Res.* **1980**, *13*, 161–169.

Summary

A comprehensive experimental and computational (B3LYP/6-31G(d)) study on the interesting solvolytic behavior of oxaspirocyclopropanated 1-norbornyl triflates has been done. Thus, the solvolysis of these easily obtained 1-norbornyl triflates, differently to the up-to-date described ones, gives place to synthetically valuable and enantiomerically pure rearranged products in good yields. Differently to the gas-phase calculations, a fair linear relationship between ln k and ΔG was obtained in the in-solution calculation. This correlation includes not only both rearranging and nonrearranging 1-norbornyl triflates, but also functionalized and nonfunctionalized ones. The scattered profile of the linear correlation in the gas-phase calculation is the result of differential unspecific solvent effects, which can be satisfactory accounted for by the PCM model in combination with the computationally inexpensive DFT B3LYP/6-31G(d) method. Hence, neither differential σ-participation nor computational artifacts are the ground for the lack of linear correlation in gas phase. Moreover, a consistent prediction of the main reaction pathways for each case has been realized by calculating the corresponding reaction barriers for the proposed competitive pathways.

Experimental Section

(1*R*,2*R*)- and (1*R*,2*S*)-3,3-Dimethylspiro[norbornane-2,2′-oxir]-1-yl Triflates [5(OTf) and 6(OTf)]. A mixture of epimeric **5(OTf)** and **6(OTf)** (44:56 by ^{1}H NMR) was obtained by standard epoxidation of (−)-fenchone-derived (1*R*)-3,3-dimethyl-2-methylenenorborn-1-yl triflate with *m*-CPBA and resolved by elution chromatography according to the procedure described previously by us.[18] **5(OTf)**. 36% yield. White solid. Mp: 41−43 °C. $[\alpha]^{20}_D$: −20.2 (0.55, CH_2Cl_2). HRMS: 285.0418 [calcd for $C_{10}H_{12}F_3O_4S$ ($M^{+\cdot}$ − CH_3), 285.0408]. ^{1}H NMR ($CDCl_3$, 200 MHz) δ: 2.85 (AB, d, J = 4.3 Hz, 1H), 2.77 (AB, d, J = 4.3 Hz, 1H), 2.60 (dm, J = 9.8 Hz, 1H), 2.21−1.72 (m, 6H), 1.00 (s, 3H), 0.98 (s, 3H) ppm. ^{13}C NMR ($CDCl_3$, 50 MHz) δ: 118.4 (c, J = 319.0 Hz, CF_3), 96.0, 69.7, 45.6, 43.3, 38.9, 37.8, 30.4, 24.2, 23.8, 23.5 ppm. FTIR (CCl_4), ν: 1414, 1207, 1132 cm^{-1}. MS *m*/*z*: 285 ($M^{+\cdot}$ − 15, 12), 167 ($M^{+\cdot}$ − Tf, 19), 151 ($M^{+\cdot}$ − TfO, 3), 137 (29), 109 (55), 85 (29), 69 (83), 67 (53), 55 (67), 43 (89), 41 (100). **6(OTf)**. 46% yield. White solid. Mp: 38−40 °C. $[\alpha]^{20}_D$: −13.5 (0.65, CH_2Cl_2). HRMS: 285.0404 [calcd for $C_{10}H_{12}F_3O_4S$ ($M^{+\cdot}$ − CH_3), 285.0408]. ^{1}H NMR ($CDCl_3$, 200 MHz) δ: 3.05 (AB, d, J = 4,4 Hz, 1H), 2.83 (AB, d, J = 4.4 Hz, 1H), 2.46 (ddd, J = 9.7 Hz, J = 3.9 Hz, J = 2.0 Hz, 1H), 2.24 (dd, J = 10.0 Hz, J = 2.0 Hz, 1H), 2.24−1.79 (m, 5H), 1.08 (s, 3H), 0.87 (s, 3H) ppm. ^{13}C NMR ($CDCl_3$, 50 MHz) δ: 118.2 (c, J = 319.0 Hz, CF_3), 97.2, 70.9, 49.5, 43.5, 38.1, 38.0, 27.3, 27.2, 24.3, 21.1 ppm. FTIR (CCl_4) ν: 1410, 1209, 1146 cm^{-1}. MS *m*/*z*: 285 ($M^{+\cdot}$ − 15, 18), 167 ($M^{+\cdot}$ − Tf, 21), 151 ($M^{+\cdot}$ − TfO, 3), 137 (32), 109 (34), 95 (15), 85 (28), 69 (84), 55 (68), 43 (91), 41 (100).

(1*R*,2*R*)- and (1*R*,2*S*)-7,7-Dimethylspiro[norbornane-2,2′-oxir]-1-yl Triflates [7(OTf) and 8(OTf)]. As described above for **5(OTf)** and **6(OTf)**, a mixture of epimeric **7(OTf)** and **8(OTf)** (23:77 by ^{1}H NMR) was obtained by epoxidation of (+)-camphor-derived

(1*S*)-7,7-dimethyl-2-methylenenorborn-1-yl triflate[22] and resolved by elution chromatography. **7(OTf)**. 17% yield. Colorless oil. $[\alpha]^{20}_D$: +3.4 (3.50, CH_2Cl_2). HRMS: 300.0633 (calcd for $C_{11}H_{15}F_3O_4S$: 300.0643). ^{1}H NMR ($CDCl_3$, 200 MHz) δ: 3.04 (AB, d, J = 4.2 Hz, 1H), 2.78 (AB, d, J = 4.2 Hz, 1H), 2.48 (m, 1H), 2.28−2.02 (m, 3H), 1.90 (d, J = 5.0 Hz, 1H), 1.84 (d, J = 14, Hz, 1H), 1.54 (m, 1H), 1.21 (s, 3H), 1.13 (s, 3H) ppm. ^{13}C NMR ($CDCl_3$, 50 MHz) δ: 118.4 (c, J = 318.8 Hz, CF_3), 98.8, 63.3, 48.7, 46.6, 38.6, 36.8, 27.5, 27.3, 18.7, 18.6 ppm. FTIR (CCl_4) ν: 1408, 1211, 1150 cm^{-1}. MS *m*/*z*: 242 ($M^{+\cdot}$−58, 2), 167 ($M^{+\cdot}$-Tf, 1), 109 (59), 81 (50), 79 (25), 69 (58), 55 (60), 43 (94), 41 (100). **6(OTf)**. 58% yield. Colorless oil. $[\alpha]^{20}_D$: −1.2 (0.13, CH_2Cl_2). HRMS: 167.1064 [calcd for $C_{10}H_{15}O_2$ ($M^{+\cdot}$ − Tf), 167.1072]. ^{1}H NMR ($CDCl_3$, 200 MHz) δ: 3.21 (AB, d, J = 4.6 Hz, 1H), 2.79 (AB, d, J = 4.6 Hz, 1H), 2.60−2.02 (m, 4H), 1.86 (dd, J = 4.6 Hz, J = 4.6 Hz, 1H), 1.66 (m, 1H), 1.59 (d, J = 13.9 Hz, 1H), 1.19 (s, 3H), 1.14 (s, 3H) ppm. ^{13}C NMR ($CDCl_3$, 50 MHz) δ: 118.2 (c, J = 318.8 Hz, CF_3), 100.7, 65.2, 53.2, 48.6, 39.1, 35.0, 27.3, 24.6, 18.7, 18.6 ppm. FTIR (CCl_4) ν: 1396, 1205, 1146 cm^{-1}. MS *m*/*z*: 167 ($M^{+\cdot}$ − Tf, 15), 137 (31), 109 (17), 93 (15), 79 (24), 69 (75), 55 (51), 43 (77), 41 (100).

(1*R*)-1-(Hydroxyacetyl)-5,5-dimethylbicyclo[2.1.1]hexane (10). Compound **10** was obtained as the unique product by solvolysis of **5(OTf)** or **6(OTf)** in 60% (w/w) aqueous ethanol buffered with triethylamine at 95.3 °C and purified by elution chromatography (silica gel, CH_2Cl_2) as described previously by us.[18] Yield: 78% from **5(OTf)** and 81% from **6(OTf)**. Colorless oil. $[\alpha]^{20}_D$: +0.8 (1.50, MeOH). HRMS: 137.0964 [calcd for $C_9H_{13}O$ ($M^{+\cdot}$ − CH_2OH), 137.0966]. For spectroscopic data, see ref 18.

(1*S*)-1-(Hydroxyacetyl)-5,5-dimethylbicyclo[2.1.1]hexane (*ent*-10). Compound ***ent*-10** was obtained, together with major product **11** (25:45 by ^{1}H NMR), by solvolysis of **7(OTf)** in 60% (w/w) aqueous ethanol buffered with triethylamine at 95.3 °C and purified by elution chromatography (silica gel, CH_2Cl_2). Yield: 18%. For spectroscopic data, see that described for **10** in ref 18.

(1*R*)-10-Hydroxyfenchone (11).[22] Compound **11** was obtained by solvolysis of **7(OTf)** (together with minority ***ent*-10**, 45:25 by ^{1}H NMR) in 60% (w/w) aqueous ethanol buffered with triethylamine at 95.3 °C or as an unique reaction product by solvolysis of **8(OTf)** under the same conditions: Purification: elution chromatography (silica gel, CH_2Cl_2/ether 4:1). Yield: 55% from **7(OTf)** and 74% from **8(OTf)**.

Acknowledgment. We thank the Ministerio de Educación y Ciencia of Spain (research project CTQ2007-67103-C02) and UCM (research projects PR34/07-15782 and PR1/08-15775) for financial support of this work. B.L.M. thanks Programa Juan de la Cierva for a research contract.

Supporting Information Available: General experimental information, optimized geometries (Cartesian coordinates), as well as ^{1}H and ^{13}C NMR spectra for the new described compounds. This material is available free of charge via the Internet at http://pubs.acs.org.

JO8009787

(22) de la Moya Cerero, S.; García Martínez, A.; Teso Vilar, E.; García Fraile, A.; Lora Maroto, B. *J. Org. Chem.* **2003**, *68*, 1451–1458.